CHEMISTRY
A European Journal

A Journal of
ChemPubSoc Europe

Accepted Article

Title: Self-Assembled Vesicle-Carbon Nanotube Conjugate Formation through Boronate-Diol Covalent Linkage

Authors: Prasanta Kumar Das, Soumik Dinda, Deep Mandal, and saheli Sarkar

This manuscript has been accepted after peer review and appears as an Accepted Article online prior to editing, proofing, and formal publication of the final Version of Record (VoR). This work is currently citable by using the Digital Object Identifier (DOI) given below. The VoR will be published online in Early View as soon as possible and may be different to this Accepted Article as a result of editing. Readers should obtain the VoR from the journal website shown below when it is published to ensure accuracy of information. The authors are responsible for the content of this Accepted Article.

To be cited as: *Chem. Eur. J.* 10.1002/chem.201703452

Link to VoR: http://dx.doi.org/10.1002/chem.201703452

Supported by
ACES

WILEY-VCH

10.1002/chem.201703452

Self-Assembled Vesicle-Carbon Nanotube Conjugate Formation through Boronate-Diol Covalent Linkage

Soumik Dinda, Deep Mandal, Saheli Sarkar and Prasanta Kumar Das*[a]

Department of Biological Chemistry, Indian Association for the Cultivation of Science, Jadavpur, Kolkata – 700 032, India

[a] S. Dinda, D. Mandal, S. Sarkar and Prof. P. K. Das
Department of Biological Chemistry
Indian Association for the Cultivation of Science
Jadavpur, Kolkata – 700032, India
Fax: +(91)-33-24732805
E-mail: bcpkd@iacs.res.in

*To whom correspondence should be addressed: bcpkd@iacs.res.in

Accepted Manuscript

This article is protected by copyright. All rights reserved.

10.1002/chem.201703452

Abstract

A vesicle-single walled carbon nanotube (CNT) conjugate is developed by boronic acid-diol covalent linkage between self-assembled vesicle and dispersed CNT. Trimesic acid based phenylboronic acid appended triple tailed amphiphiles (**T1** and **T1S**) were synthesized that formed monolayered vesicles through *H*-aggregation in DMSO-water (2:1 v/v) and pure water, respectively. Aqueous CNT dispersion was prepared with cholesterol based glucose functionalized amphiphile (**D1**). These two supramolecular self-assemblies were covalently linked using boronic acid-diol interaction between phenylboronic acid based **T1S** vesicle and 1,2-diol moieties of glucose tethered dispersing agent (**D1**) to develop vesicle-CNT conjugate. Lewis acid-base chemistry was exploited to form this boronate-diol adduct between two supramolecular self-assemblies. The formation of vesicles, CNT dispersion and the vesicle-CNT conjugate was characterized by microscopic and spectroscopic techniques. Anticancer drug doxorubicin was encapsulated within this **T1S**-vesicle-**D1**-CNT conjugate with a higher loading capacity compared to individual cargo carrier (vesicle or CNT). This cytocompatible **T1S**-vesicle-**D1**-CNT conjugate successfully delivered loaded doxorubicin within B16F10 melanoma cell and also exhibited better cellular transporation ability compared to drug loaded vesicle or CNT. This was further reflected in enhanced killing efficiency of the cancer cells by vesicle-CNT conjugate compared to drug loaded vesicle or CNT.

Accepted Manuscript

This article is protected by copyright. All rights reserved.

Introduction

Over the past few decades, lipid vesicles gained enormous importance because of its ability to mimic the properties of biological membranes and cellular organelles.[1,2] Vesicle, a unique class of supramolecular self-assembly, is an well established drug delivery vehicle with considerable cargo loading ability, excellent cytocompatibility and biodegradability.[3-5] Concurrently, in recent years, single walled carbon nanotube (CNT) has also emerged as succesful cellular transporter due to its needle like hollow shape and superior ability to translocate through plasmatic membrane.[6] CNT, the pseudo one dimensional allotrope of carbon, has been widely exploited in numerous scientific fields due to its intrinsic mechanical, thermal and optical properties.[7,8] Both vesicles and CNTs have their individual prominence in supramolecular self-assembly and biomedicine. Despite having such extraordinary credentials, the major limitations of using CNTs as drug delivery vehicle are poor cargo loading ability and inherent cytotoxicity to mammalian cells.[9] Moreover, the hydrophobic surface of CNTs non-specifically binds with the nutrients (essential constituents for cell growth) leading to indirect toxicity towards living cells.[9c] On the contrary, the major drawback of vesicles is its fast elimination from blood circulation due to efficient uptake by reticulo-endothelial system.[10] Some pegylated lipids (stealth liposomes) had overcome this problem where polyethylene glycol (PEG) moiety acts as the steric stabilizer.[10] However, this sterically stabilized vesicle often prevented while entering into the targeted cells.[3a]

To overcome these hurdles, necessity of developing a new soft-nanocomposite has emerged with low cytotoxicity and improved drug loading ability. To this end, amalgamation of self-assembled vesicles with dispersed CNT may lead to the development of vesicle-CNT conjugate with desired features. Till date, very few attempts were made to develop CNT-liposome conjugates. Regev and co-workers reported the formation of CNT-liposome conjugate through covalent amide linkage between carboxylated multi-walled CNT and the

This article is protected by copyright. All rights reserved.

Accepted Manuscript

primary amine containing liposome.[11] CNT-liposome conjugate was also utilized as molecular-transporter by utilizing the ligand-receptor interaction between liposome and CNT.[7b] Electrostatic interaction had also been used to form single walled carbon nanotube-liposome complex.[12] Also there are reports on the formation of CNT mediated fusion of lipid vesicles, vesicle encapsulated multi-walled CNT.[13] However, the befitting role of the vesicle-CNT conjugate over the individual cargo carrier (vesicle or CNT) is yet to be emphasized.

Herein, the vesicle-CNT conjugate was constructed using covalent interaction between the CNT dispersing agent and vesicular building blocks. Phenylboronic acid appended trimesic acid based monolayered vesicles (**T1S**) were linked with the cholesterol based glucose functionalized CNT dispersing agent (**D1**) using complementary boronic acid-diol interaction chemistry (Scheme 1, Figure 1a). The lewis acid-base interaction was exploited to make the covalent linkage between the building block of monlayered vesicles and CNT dispersing agent to develop the vesicle-CNT conjugate. To the best of our knowledge, this is the first ever approach where dispersed CNT surface has been decorated with monolayered vesicles. Microscopic and spectroscopic techniques were utilized to characterize this newly developed vesicle-CNT conjugate. The vesicle-CNT conjugate was found to be stable and cytocompatible in biological milieu. Anticancer drug doxorubicin was encapsulated within this vesicle-CNT conjugate with improved loading capacity compared to its individual constituents. Importantly, vesicle CNT conjugate delivered the drug with greater efficiency inside the B16F10 melanoma cells compared to drug loaded individual vesicle or dispersed CNT resulting in higher killing of cancer cells by the conjugate.

Results and Discussion

A trimesic acid based triskelion amphiphile (**T1**) was synthesized having three phenylboronic acid (PBA) moieties at the terminals (Figure 1a). C3-symmetrical trimesic acid was chosen as

This article is protected by copyright. All rights reserved.

Accepted Manuscript

a primary scaffold because of its tri-functionalized structure with aromatic moiety at its core that could instigate ordered π-π stacking during self-assembly. The PBA moieties were integrated through oxyethylene spacer at the terminals of **T1** to impart hydrophilicity in the amphiphile.[14,15] With the objective to develop vesicle-CNT conjugate, a cholesterol based glucose functionalized CNT dispersing agent (**D1**, Figure 1a) was synthesized.[16] The 1,2-diol moieties of glucose unit of **D1** would be appropriate for linking with boronic acid of vesicular building block via boronate-diol covalent interaction.[17] Compound-**T1** was found to be insoluble in water while it formed a translucent solution in DMSO-water (2:1 v/v) binary solvent mixture with an indication of vesicle formation. The corresponding transmission electron microscopic (TEM) image showed the formation of spherical vesicular self-assemblies having average diameter of 150-200 nm (Figure 1b). Since **T1** formed vesicle in DMSO-water binary solvent mixture, we synthesized the sodium salt of **T1** (**T1S**, Figure 1a) with the expectation that it will form vesicle in pure aqueous medium. Indeed, **T1S** formed translucent solution in water with a preliminary indication of vesicle formation. The respective TEM image also confirmed the formation of vesicular aggregates in water with comparatively smaller diameter (50-100 nm, Figure 1c). Both vesicular self-assemblies (originating from **T1** and **T1S**) bear common morphological characteristics of thin wall with a hollow core.

Critical Aggregation Concentration (CAC).

The critical aggregation concentration (CAC) of **T1** and **T1S** was measured for both amphiphiles by surface tension method in the respective solvent systems. The gradual decrease of surface tension upon increasing the concentrations of **T1** and **T1S** continued until reaching the CAC values. After attainment of the CAC value, any further addition of amphiphile molecules will just increase the number of aggregation without any substantial

This article is protected by copyright. All rights reserved.

Accepted Manuscript

change in surface tension values. The CAC values were found to be ~250 and ~300 µg/mL for **T1** and **T1S**, respectively (Figure S1 in the Supporting Information).

Microscopic Studies.

Field-emission scanning electron microscopic (FESEM) images showed the formation of vesicular self-assemblies by **T1** and **T1S** in respective solvents having average diameter of 150-200 nm and 50-100 nm, respectively (Figure 2a,b). In concurrence with the FESEM images, atomic force microscopy (AFM) further ensured the perfectly spherical morphology formed by the self aggregation of **T1** and **T1S** in respective solvent systems (Figure 2c,d). AFM images showed the average diameter of **T1** vesicles were in the range of ~200 nm while that was ~90 nm for **T1S** vesicles. Moreover, the cross-section analysis of the AFM images (Figure 2c (p-q) and 2d (r-s)) provide an idea about the height of the vesicles which was ~30 nm and ~15 nm for **T1** and **T1S** vesicles, respectively (Figure 2e and 2f) indicating that both the vesicles were hollow and flattened in shape.[18]

Spectroscopic Studies.

Dynamic Light Scattering (DLS) and Zeta (ζ) Potential Measurements.

The dynamic light scattering (DLS study) revealed the mean hydrodynamic diameter of both vesicles. In Figure 2g, size distribution profile for **T1** delineates the average hydrodynamic diameter for **T1** vesicles is ~150 nm while it is quite smaller for **T1S** vesicles (~80 nm). These spectroscopic data regarding the size of both the vesicular aggregates (**T1** and **T1S**) is in well agreement with the microscopic evidences.

The colloidal stability of **T1** and **T1S** was estimated by zeta (ζ) potential measurement. Very high ζ potential value in case of **T1S** (-22.91 mV) compared to **T1** (-3.7 mV) is probably due to negatively charged boronate ion in the side chains of **T1S**. These values indicate substantial stability of the corresponding vesicular aggregates.[19]

This article is protected by copyright. All rights reserved.

Accepted Manuscript

Solvent Dependent ^{1}H NMR Study. To know the various interacting forces responsible for the formation of supramolecular self-assemblies, the solvent dependent ^{1}H-NMR experiment was performed for both amphiphiles (**T1** and **T1S**). The NMR signals of aromatic protons gradually upfield shifted with reduced peak intensity upon transformation from non-self-assembled state (**T1** and **T1S** taken in DMSO-d6) to self-assembled state (**T1** taken in DMSO-d6-D_2O (2:1 v/v) and **T1S** taken in D_2O) of the amphiphiles (Figure 3a,b). In DMSO-d6, the aromatic proton of central trimesic acid of **T1** showed a sharp peak at δ = 8.42 ppm while the aromatic protons of PBA moieties showed distinguished peaks at the region δ = 7.89 ppm and δ =7.92-8.13 ppm and 6.88-6.95 ppm, respectively. In DMSO-d6, **T1** was present in molecularly dissolved state without any self-association. Upon increasing the D_2O content, the peaks stated above got shifted in the upfield region i.e. at δ = 7.89 ppm and δ =7.39-7.62 ppm and 6.51-6.59 ppm, respectively accompaning with reduced peak intensities. In a similar fashion, the NMR signals of aromatic protons of trimesic acid of **T1S** got upfield shifted form δ = 8.80 ppm to δ = 8.28 ppm on moving form non-self-assembled state (in DMSO-d6) to self-assembled state (in D_2O). Notably, the aromatic protons of PBA moieties exhibited upfield shifting of the NMR signals from δ =7.81-8.07 ppm and 7.81-7.88 ppm to δ =7.41-7.62 ppm and 6.41-6.48 ppm, respectively. Thus, self-aggregation gets started and facilitated during the increment of D_2O content. This result delineates the active participation of hydrophobic interaction and π-π stacking during vesicle formation during self-assembly of **T1** and **T1S**.[15b]

Steady State Fluorescence Anisotropy.

Steady state fluorescence anisotropy (*r*) measurement was carried out using 1,6-diphenyl-1,3,5-hexatriene (DPH) as probe to find out the nature of microenvironment in self-aggregated structure. The *r*-value increased from 0.08 to 0.19 and 0.07 to 0.15 (Table 1) for DPH included **T1** and **T1S** self-assemblies over a concentration range from 2 to 20 mg/mL,

This article is protected by copyright. All rights reserved.

Accepted Manuscript

respectively. The significantly higher *r* values (greater restriction in the movement of DPH in the hydrophobic region) of DPH (0.19 for **T1** and 0.15 for **T1S**) compared to that of micellar aggregates of sodium dodecyl sulfate (r = 0.054) further confirm the formation of vesicular aggregates by **T1** and **T1S**.[20]

UV-vis Study.

The supramolecular aggregation pattern of **T1** and **T1S** was investigated from UV-vis spectroscopy in the presence of well known chromophore, 8-anilino-1-naphthalenesulfonic acid (ANS) (1×10^{-5} M). ANS is prone to confine itself at the hydrophobic region of the aggregated structure. It showed absorption maxima at 380 and 378 nm in non-self-assembled state of **T1** and **T1S** (both were taken in DMSO), respectively. With increasing the water content the absorption maxima of ANS gradually blue shifted for both amphiphiles indicating the initiation of self-aggregation of monomeric units. In self-aggregated state of **T1** (DMSO-H_2O (2:1 v/v)) and **T1S** (water)**,** the absorption maxima of ANS was shifted to 367 and 345, respectively (Figure 3c,d). This blue shift in absorption maxima of ANS during self-aggregation designates parallel plane-to-plane stacking of the amphiphiles forming a sandwich type arrangement (*H*-type aggregation).[14b,21] However, no such change in absorption and aggregation pattern is known to be reported for bilayered phosphocholine (PC) liposomes.[14b] Thus, a monolayered ordered arrangement of **T1** and **T1S** possibly took place due to the hydrophilic−hydrophobic−hydrophilic molecular backbone of the amphiphiles, which is different in nature from that of bilayered PC liposomes.[14b,22] The X-ray diffraction (XRD) of **T1** and **T1S** in self-aggregated state showed the broad peak at 2θ ~23° (Figure S2 in the Supporting Information), which corresponds to π–π stacked organization of amphiphiles.[23]

Development of Vesicle-CNT Conjugate.

This article is protected by copyright. All rights reserved.

Accepted Manuscript

10.1002/chem.201703452

At this point, we intend to amalgamate the newly developed vesicles with dispersed CNTs to fabricate vesicle-CNT conjugate. Cholesterol based glucose tailored amphiphile (**D1**, Figure 1a) debundled the amphiphobic CNT with 63% efficiency (Figure S3a in the Supporting Information) in water (see experimental section). The hydrophobic cholesteryl moiety of **D1** possibly got attached non-covalently on the CNT surface and the hydrophilic glucose unit facilitated the dispersion of hydrophobic CNTs in aqueous medium. This CNT dispersion was found to be stable more than 3 months without any precipitation. The debundling of CNT was confirmed from the corresponding TEM image (Figure 1d) where individual nanotubes having a diameter of 5-7 nm and average length of 400-600 nm were well separated from each other. Furthermore, Raman spectroscopic investigation was carried out to characterize the aqueous dispersion of CNT by **D1**. The sharp G-band at 1590 cm^{-1} was observed in the Raman spectrum due to the tangential C-C stretching transitions in CNT (Figure S4a in the Supporting Information).[24] Moreover, other two peak at 1350 cm^{-1} and 2690 cm^{-1} were found in the Raman spectrum corresponding to the D-band and its second-order G'-band respectively (Figure S4a in the Supporting Information).[24] All the above bands corroborate with the Raman spectrum of solid pristine CNT (Figure S4b in the Supporting Information). The aqueous dispersion of CNT (**D1**) was mixed with the preformed vesicles of **T1S** to fabricate vesicle-CNT conjugate (see experimental section). As to our expectation, the TEM image of the mixed solution (**T1S**-vesicle + **D1**-CNT dispersion) confirmed the successful formation of **T1S**-vesicle-**D1**-CNT conjugate (Figure 4a and Figure S5 in the Supporting Information). The vesicles were found to be aligned over the CNT surface and the shape and the size of the vesicles were found to be unchanged after conjugation with CNT. The vesicles get attached on the CNT surface through lewis acid-base chemistry where boronate unit of the vesicular building block acts as lewis acid and 1,2-diol of the glucose unit on the CNT surface acts as lewis base.[17] The formation of cyclic boronate-diol adduct through covalent

This article is protected by copyright. All rights reserved.

Accepted Manuscript

linkage between building block of vesicles (**T1S**) and dispersing agent of CNT (**D1**) was characterized by ^{1}H-NMR and mass spectroscopy (Figure S6 and S7 in the Supporting Information). This covalent linkage tied up both vesicle and CNT leading to formation of **T1S**-vesicle-**D1**-CNT conjugate. Corresponding AFM images (Figure 4b) also supported the attachment of vesicles on CNT surface confirming the successful conjugation of vesicle with CNTs. Importantly, vesicle-CNT conjugate suspension was found to be stable in water (Figure S3b in the Supporting Information). Thus, the conjugation between self-assembled vesicle and dispersed CNT did not affect the structural integrity of the vesicle as well as the non-covalent attachment of dispersing agent on CNT surface, otherwise CNT would have been precipitated. The vesicle-CNT conjugate formation was further characterized by thermogravimetric analysis (TGA). To this end, TGA plot of **D1**-CNT showed a sharp decrease in weight between 200 and 300 °C corresponding to the decomposition of **D1** (Figure 4c). Similarly, TGA plot of **T1S**-vesicle-**D1**-CNT conjugate exhibited sharp decrease in weight between 100 and 200 °C corresponding to the decomposition of newly formed boronate-diol cyclic conjugate (Figure 4d). Almost 35% and 38% residue remains after the decomposition which is corresponding to the amount of CNT present in the sample in case of **D1**-CNT and **T1S**-vesicle-**D1**-CNT conjugate, respectively (Figure 4c,d). Hence, ~65% of the **D1** dispersing agent gets attached to the walls of the CNT while ~62% of the cyclic adduct (**D1**-**T1S**) was involved in the formation of vesicle-CNT conjugate.

To ensure the formation of vesicle-CNT conjugate between **T1S**-vesicle and **D1**-CNT, control experiment was carried out where CNT was debundled with a well-known dispersing agent SDBS (sodium dodecyl benzenesulfonate) and mixed with preformed vesicular solution of **T1S (**Figure S8a in the Supporting Information). In another experiment, monolayered vesicle of a triskelion amphiphile devoid of PBA moiety was mixed with aqueous dispersion of **D1**-CNT by (Figure S8b in the Supporting Information).[14b] In both

This article is protected by copyright. All rights reserved.

Accepted Manuscript

cases, corresponding TEM images (Figure S8c, S8e and S8d, S8f in the Supporting Information) did not provide any indication on the formation of vesicle-CNT conjugate. Similarly, the AFM images did not exhibit any attachment of vesicles to the CNT surfaces (Figure S8g and S8h in the Supporting Information). These control experiments further confirmed that covalent bond formation between complementary boronate-diol moieties of vesicle and CNT dispersing agent led to the formation of new vesicle-CNT conjugate.

The conjugation of vesicles on dispersed CNT surfaces was also investigated by photoluminescence spectroscopy. We have studied the emission property of fluorescein isothiocyanate (FITC) in **T1S** vesicle, **T1S**-vesicle-**D1**-CNT conjugate and water. FITC is known to get localized at the hydrophobic core of the aggregated structure.[25] Concurrently, CNT is also well known for quenching the emission intensity of the fluorescence probe (FITC).[26] FITC exhibited emission maxima at 520 nm upon excitation at 495 nm (Figure 5a). In **T1S** vesicle, a significant increase in the FITC fluorescence intensity was noted obviously due to its localization at the hydrophobic wall of the monolayered vesicles. Notably, the fluorescent intensity of FITC gets quenched drastically in the **T1S**-vesicle-**D1**-CNT conjugate (Figure 5a), which confirms the presence of CNT in close proximity of the probe, located at the hydrophobic vesicular wall. Hence it further validates the formation of **T1S**-vesicle-**D1**-CNT conjugate by the attachment **T1S** vesicle on the surface of dispersed CNT, which is in concurrence with microscopic evidences.

Moreover, we measured the decay time of coumarin 153 (C153, excitation 405 nm) in **T1S** vesicle, **T1S**-vesicle-**D1**-CNT conjugate as well as in water in the time-correlated single-photon counting (TCSPC) experiment monitored at 550 nm (Figure 5b). The decay time of free C153 in water was found to be 1.63 ns while it increased to 1.71 ns when the dye was included within **T1S** vesicle. However, the decay time observed in **T1S** vesicle is distinctly lower than that was reported for bilayered PC liposomes (4.65 ns), which further

This article is protected by copyright. All rights reserved.

Accepted Manuscript

indicates the formation of monolayered vesicles by **T1S**.[14b] This increment in decay time of C153 within **T1S** vesicle was possibly due to the encapsulation of the dye in more hydrophobic environment. Importantly, the decay time of C153 further increased to 1.93 ns within **T1S**-vesicle-**D1**-CNT conjugate. Thus, **T1S**-vesicle-**D1**-CNT conjugate possessed enhanced hydrophobic microenvironment compared to **T1S** vesicle presumably due to the attachment of monolayered vesicles on the surface of hydrophobic CNT. All spectroscopic and microscopic evidences ensured that the boronate-diol covalent interaction between the vesicular amphiphiles and CNT dispersing agent led to the development of **T1S**-vesicle-**D1**-CNT conjugate.

Doxorubicin Loading and Release.

After ensuring the successful formation of **T1S**-vesicle-**D1**-CNT conjugate, we aim to investigate the cargo loading ability and cellular transportation efficacy of this conjugate. To this end, anticancer drug doxorubicin was separately loaded in the **T1S** vesicle, aqueous CNT dispersion (**D1**) as well as **T1S**-vesicle-**D1**-CNT conjugate (see experimental section). Free doxorubicin was discarded from the loaded doxorubicin in vesicle and **T1S**-vesicle-**D1**-CNT conjugate by size exclusion column chromatography using sephadex G-50. In case of CNT, free doxorubicin was separated after precipitating the drug loaded CNT through centrifugation (see experimental section). The eluted solution from the sephadex column showed characteristic UV-vis absorbance peaks at λ_{max} = 490 nm indicating the presence of the doxorubicin within the drug carriers (Figure 6a). Drug encapsulated vesicle and **T1S**-vesicle-**D1**-CNT solutions were further observed under fluorescence microscope, which showed bright red emitting spherical aggregates (Figure 6b,c). This observation subsequently confirmed the loading of doxorubicin within vesicle and **T1S**-vesicle-**D1**-CNT conjugate. Encapsulation of the drug was further ensured by comparing the fluorescence intensity of free doxorubicin and loaded doxorubicin in different drug carriers (vesicle, CNT and **T1S**-vesicle-

This article is protected by copyright. All rights reserved.

Accepted Manuscript

D1-CNT conjugates) at 590 nm (λ_{ex}= 490 nm) (Figure S9 in the Supporting Information). The emission intensity of loaded doxorubicin in each carrier (**T1S**-vesicle, **D1**-CNT and **T1S**-vesicle-**D1**-CNT) was found to be very low compared to that of free doxorubicin at same concentration (Figure S9 in the Supporting Information).[14b] Notably, encapsulated doxorubicin regained its fluorescence intensity and became comparable to free doxorubicin upon treating the drug loaded, **T1S**-vesicle with Triton X-100, **D1**-CNT with 1(N) HCl and **T1S**-vesicle-**D1**-CNT conjugate with both Triton X-100 and 1(N) HCl (Figure S9 in the Supporting Information). Triton X-100 assisted the rupturing of vesicular wall resulting in release of the drug.[27] Protonation of the $-NH_2$ group of doxorubicin in presence of HCl resulted in the release of hydrophilic drug from CNT surface due to the lower affinity of the drug towards the hydrophobic CNT surface.[28] Triton X-100 and 1(N) HCl both have cumulative effect on doxorubicin loaded **T1S**-vesicle-**D1**-CNT conjugate for releasing the drug. Photoluminiscence spectroscopy further confirmed the drug loading ability of different cargo transporters.

Doxorubicin loading efficiency of the **T1S**-vesicle-**D1**-CNT conjugate was found to be ~67% whereas in case of individual **T1S**-vesicle and **D1**-CNT, it was ~57% and ~23%, respectively (measured after treating the doxorubicin entrapped **T1S**-vesicle with Triton X-100, **D1**-CNT with 1(N) HCl and **T1S**-vesicle-**D1**-CNT conjugate with both Triton X-100 and 1(N) HCl, followed by comparing the absorbance of released doxorubicin with standard calibration curve, see experimental section, Figure S10 in the Supporting Information).[29] **T1S**-vesicle is capable to accommodate considerable amount of doxorubicin in its inner aqueous core, while CNT can upload doxorubicin to its side wall through hydrophobic interaction. In **T1S**-vesicle-**D1**-CNT conjugate, combined presence of the aqueous core of vesicle and large CNT surface resulted a synergistic contribution towards the notable improvement in the drug loading efficiency compared to the individual constituents.

This article is protected by copyright. All rights reserved.

Accepted Manuscript

Media Stability.

Prior to utilize this newly developed **T1S**-vesicle-**D1**-CNT conjugate as a delivery vehicle, we tested the stability of this conjugate in biological milieu as well its cytocompatibility against the mammalian cells. According to the visual appearance and suspension stability index, vesicle-CNT conjugate ([CNT] = 25 μg/mL) in Dulbecco's Modified Eagles' Medium (DMEM) with varying fetal bovine serum (FBS) concentration was found to be more than 90% stable (Figure S11a in the Supporting Information). Moreover, the conjugate also exhibited significant stability (>90%) up to 10 days in both DMEM media supplemented with 10% FBS as well as in physiological pH *i.e.* pH 7.4 PBS buffer (Figure S11b,c in the Supporting Information). Ensuring high media stability of **T1S**-vesicle-**D1**-CNT, the cytocompatibility of **T1S** vesicle, dispersed (**D1**) CNT and **T1S**-vesicle-**D1**-CNT conjugate was investigated against the B16F10 mammalian cell line by MTT assay (Figure S12 in the Supporting Information).[30] The **T1S** vesicle (100-500 μg/mL) showed a superior cytocompatibility having 90-95% viable cells after 12h of incubation. In case of dispersed (**D1**) CNT (5-25 μg/mL), moderate cell viability (~40-60%) was noted presumably due to the inherent toxicity and adverse effect on the necessary cellular nutrients by CNT (Figure S12 in the Supporting Information).[9] Interestingly **T1S**-vesicle-**D1**-CNT conjugates with similar CNT concentration range (5-25 μg/mL), exhibited substantial cytocompatibility where ~70-80% cells were found to be alive (Figure S12 in the Supporting Information). The inclusion of highly cytocompatible vesicular aggregates on the surface of CNT significantly reduced the toxic effect of CNT in the **T1S**-vesicle-**D1**-CNT conjugate and satisfied its suitability as cellular transporter.

Internalization of Doxorubicin within Cancer Cells.

Herein, drug transportation ability by individual delivery vehicle was investigated upon incubation of doxorubicin (5 μg/mL) loaded **T1S**-vesicle, **D1**-CNT and **T1S**-vesicle-**D1**-CNT

This article is protected by copyright. All rights reserved.

Accepted Manuscript

conjugate, separately with B16F10 melanoma cells for 6 h. In each instance, bright red fluorescence image of cells under the fluorescence microscope confirmed the successful internalization of doxorubicin inside B16F10 melanoma cells (Figure 7a,b,d,e,g,h). The acidic microenvironment of B16F10 cancer cells might have facilitated the protonation of the $–NH_2$ group of doxorubicin and successecsive release of drug from hydrophobic CNT surface. The extent of doxorubicin internalization within B16F10 cells by different delivery vehicle was assessed by flow cytometric analysis. The respective flow cytometric plot exhibited fluorescence intensity in the order of 10^4–10^5 having mean fluorescence value of 29295, 39333 and 82860 for doxorubicin loaded **T1S**-vesicle, **D1**-CNT and **T1S**-vesicle-**D1**-CNT conjugate, respectively (Figure 7c,f,i). It is evident that dispersed CNT has better cargo transportation ability than the vesicle. This observation is in concurrence with previous report that despite having higher loading capacity, vesicle has the poor internalization efficacy in contrast to the CNT.[31,32] Importantly, with the objective of the present study, most efficient drug delivery was exhibited by **T1S**-vesicle-**D1**-CNT conjugate having highest mean fluorescence value of 82860 (Figure 7i). Thus, in comparison to the individual vesicle and CNT, the newly developed **T1S**-vesicle-**D1**-CNT conjugate is more proficient towards transporting the anti-cancer drug doxorubicin inside the B16F10 cancer cells primarily due to the amalgamation of vesicles and CNT having high drug loading capacity and efficient cell penetration ability, respectively.

Cancer Cell Killing.

The superior cellular transportation ability of **T1S**-vesicle-**D1**-CNT conjugate prompted us to investigate the efficacy of the delivered doxorubicin towards killing the cancer cells. Herein, we studied the % killing of B16F10 cells for doxorubicin loaded delivery vehicles by MTT assay. B16F10 cells were treated for 12 h with doxorubicin loaded (5-25 μg/mL) **T1S**-vesicle, **D1**-CNT and **T1S**-vesicle-**D1**-CNT conjugate, separately (Figure 7j). In each

This article is protected by copyright. All rights reserved.

Accepted Manuscript

instance, the killing efficacy almost steadily increased with increase in concentration of doxorubicin from 5 to 25 μg/mL. Also, at a given concentration of doxorubicin, the % killing of cancer cells distinctly improved from vesicle to CNT and being most efficient for **T1S**-vesicle-**D1**-CNT conjugate. Encouragingly, drug loaded **T1S**-vesicle-**D1**-CNT conjugate showed ~71% killing of B16F10 cells at [doxorubicin] = 25 μg/mL, whereas drug loaded native vesicle and dispersed CNT exhibited 44% and 49% killing of cancer cells, respectively (Figure 7j). In case of free doxorubicin, only ~21% killing of B16F10 cells was observed at 25 μg/mL of the drug upon 12 h of incubation (Figure S13 in the Supporting Information). This indicates the inefficient killing ability of free doxorubicin without any cargo transporter. Cancer cell killing efficiency by doxorubicin loaded different delivery vehicles follows the same trend that was observed in the flow cytometry (**T1S**-vesicle-**D1**-CNT conjugate is being the most efficient). Hence, the amalgamation of vesicle and CNT through boronate-diol covalent interaction leads to the development of a highly efficient delivery vehicle (**T1S**-vesicle-**D1**-CNT conjugate) which has improved drug loading ability and notable proficiency in cellular transportation.

Conclusions

In summary, the vesicle-CNT conjugate was developed with facile combination of supramolecular self-assemblies of phenylboronic acid appended trimesic acid based monolayered vesicles (**T1S**) and cholesterol based glucose functionalized CNT dispersion (**D1**) using boronate-diol covalent linkage. Formation of this soft-nanocomposites was thoroughly investigated using different microscopic as well as spectroscopic techniques. Anticancer drug doxorubicin was encapsulated within this vesicle-CNT conjugate with improved loading capacity compared to its individual constituents. This newly developed conjugate efficiently delivered the drug inside the B16F10 melanoma cells in comparison to only vesicle/CNT resulting in higher killing of cancer cells. The present study may instigate a

This article is protected by copyright. All rights reserved.

Accepted Manuscript

novel strategy towards developing smart delivery vehicle with regulated dose of loaded drug and improved proficiency in cellular transportation.

Acknowledgements:

P.K.D. is thankful to CSIR, India (ADD, CSC0302) for financial assistance. S.D., D.M. acknowledge CSIR, India and S.S thanks DST inspire for Research Fellowships. We acknowledge Dr. Moumita Ghosh for helpful discussion.

Supporting Information Available: Experimental procedures, ^{1}H-NMR and mass spectral analysis of the amphiphiles, synthetic scheme, critical aggregation concentration (CAC) plot**,** XRD plot, Raman spectra, ^{1}H-NMR and mass spectra of boronate-diol adduct, visual observations of **D1**-CNT and **T1S**-vesicle-**D1**-CNT conjugate in water, control experiment by mixing of **T1S**-vesicle and CNT dispersed by SDBS and another triskelion vesicle and **D1**-CNT and the corresponding TEM and AFM images, photoluminescence spectra of doxorubicin loaded **D1**-CNT, **T1S**-vesicle**, T1S**-vesicle-**D1**-CNT conjugate and the release of doxorubicin, UV-Vis spectra of released doxorubicin from **T1S**-vesicle-**D1**-CNT conjugate, **T1S**-vesicle and **D1**-CNT, suspension stability index of **T1S**-vesicle-**D1**-CNT conjugate, cell viability data, killing of B16F10 cells by free doxorubicin. Supporting information for this article is available on the website under http://www.chemeurj.org/ or from the author.

References:

[1] a) D. A. Wilson, R. J. M. Nolte, J. C. M. van Hest, *J. Am. Chem. Soc.* **2012**, *134*, 9894−9897; b) P. Walde, K. Cosentino, H. Engel, *ChemBioChem* **2010**, *11*, 848-865;

[2] a) H. T. Jung, B. Coldren, J. A. Zasadzinski, D. J. Iampietro, E. W. Kaler, *Proc. Natl. Acad. Sci.* **2001**, *98*, 1353-1357; b) Y. X Xu, G. T. Wang, X. Zhao, X. K. Jiang, Z. T. Li, *Langmuir* **2009**, *25*, 2685-2688.

[3] a) A. A. Gabizon, *Adv. Drug Deliv. Rev.* **1995**, *16*, 285-294; b) P. Majumder, S. Bhunia, J. Bhattacharyya, A. Chaudhuri, *J. Control. Release* **2014**, *180*, 100-108.

This article is protected by copyright. All rights reserved.

Accepted Manuscript

[4] a) D. Zucker, D. Marcus, Y. Barenholz, A. Goldblum, *J. Control. Release* **2009**, *139*, 73-80; b) D. Pramanik, B. K. Majeti, G. Mondal, P. P. Karmali, R. Sistla, O. G. Ramprasad, G. Srinivas, G. Pande, A. Chaudhuri, *J. Med. Chem.* **2008**, *51*, 7298-7302.

[5] a) K. Kono, *Adv. Drug Deliv. Rev*. **2001**, *53*, 307-319; b) M. H. Gaber, K. Hong, S. K. Huang, D. Papahadjoponlos, *Pharm. Res.* **1995**, 12, 1407-1416.

[6] a) D. Pantarotto, R. Singh, D. M. Carthy, M. Erhardt, J. P. Briand, M. Prato, K. Kostarelos, A. Bianco, *Angew. Chem. Int. Ed*. **2004**, *43*, 5242-5246; *Angew. Chem.* **2004**, *116*, 5354-5358; b) D. Tasis, N. Tagmatarchis, A. Bianco, M. Prato, *Chem. Rev.* **2006**, *106*, 1105-1136; c) S. Dhar, Z. Liu, J. Thomale, H. J. Dai, S. J. Lippard, *J. Am. Chem. Soc.* **2008**, *130*, 11467-11476.

[7] a) S. Iijima, Nature **1991**, 354, 56-58; b) E. Miyako, K. Kono, E. Yuba, C. Hosokawa, H. Nagai, Y. Hagihara, *Nat. Commun.* **2012**, *3*, 1-9; c) S. Brahmachari, D. Das, A. Shome, P. K. Das, *Angew. Chem. Int. Ed*. **2011**, *50*, 11243-11247; *Angew. Chem.* **2011**, *123*, 11439-11443;

[8] a) B. G. Cousins, A. K. Das, R. Sharma, Y. Li, J. P. McNamara, I. H. Hillier, I. A. Kinloch, R. V. Ulijn, *Small* **2009**, *5*, 587-590; b) E. Miyako, T. Itho, Y. Nara, T. Hirotsu, *Chem. Eur. J.* **2009**, *15*, 7520-7525.

[9] a) R. Wang, C. Mikoryak, S. Li, D. Bushdiecker, I. H. Musselman, P. Pantano, R. K. Draper, *Mol. Pharmaceutics* **2011**, *8*, 135-1361; b) K. Kostarelos, *Nat. Biotechnol.* **2008**, *26*, 774-776; c) A. Casey, E. Herzog, F. M. Lyng, H. J. Byrne, G. Chambers, M. Davoren, *Toxicol. Lett.* **2008**, *179*, 78-84.

[10] a) A. Gabizon, H. Shmeeda, Y. Barenholz, *Clin. Pharmacokinet.* **2003**, *42*, 419-436; b) A. L. Klibanov, K. Maruyama, A. M. Beckerleg, V. P. Torchilin, L. Huang, *Biochim. Biophys. Acta, Biomembr*. **1991**, *2*, 142-148.

[11] F. Karchemski, D. Zucker, Y. Barenholz, O. Regev, *J. Control. Release* **2012**, *160*, 339-345.

This article is protected by copyright. All rights reserved.

Accepted Manuscript

[12] T. Kim, C. Do, S. Kang, M. Lee, S. Lim, S. Choi, *Soft Matter* **2012**, *8*, 9073-9078.

[13] a) R. M. Bhaskara, S. M. Linker, M. Vo¨gele, J. Ko¨finger, G. Hummer, *ACS Nano* **2017**, *11*, 1273-1280; b) P. Zou, G. Shi, C. Y. Pan, *J. Polym. Sci. A Polym. Chem.* **2009**, *47*, 3669–3679.

[14] a) C. M. A. Leenders, M. B. Baker, I. A. B. Pijpers, R. P. M. Lafleur, L. Albertazzi, A. R. A. Palmans, E. W. Meijer, *Soft Matter* **2016**, *12*, 2887-2893; b) S. Dinda, M. Ghosh, P. K. Das, *Langmuir* **2016**, *32*, 6701-6712; c) A. Heeres, C. van der Pol, M. Stuart, A. Friggeri, B. L. Feringa, J. van Esch, *J. Am. Chem. Soc.* **2003**, *125*, 14252-14253.

[15] a) C. M. A. Leenders, G. Jansen, M. M. M. Frissen, R. P. M. Lafleur, I. K. Voets, A. R. A. Palmans, E. W. Meijer, *Chem. Eur. J.* **2016**, *22*, 4608–4615; b) P. Besenius, K. P. van den Hout, H. M. H. G. Albers, T. F. A. de Greef, L. L. C.Olijve, T. M. Hermans, B. F. M. de Waal, P. H. H. Bomans, N. A. J. M. Sommerdijk, G. Portale, A. R. A. Palmans, M. H. P van Genderen,. J. A. J. M. Vekemans, E. W. Meijer, *Chem. Eur. J.* **2011**, *17*, 5193-5203.

[16] D. Mandal, S. Dinda, P. Choudhury, P. K. Das, *Langmuir* **2016**, *32*, 9780-9789.

[17] a) W. L. A. Brooks, B. S. Sumerlin, *Chem. Rev.* **2016**, *116*, 1375-1397; b) Y. Kubo, R. Nishiyabu, T. D. James, *Chem. Commun.* **2015**, *51*, 2005-2020.

[18] I. Reviakine, A. Brisson, *Langmuir* **2000**, *16*, 1806-1815.

[19] E. Chibowski1, A. Szczes, *Adsorption* **2016**, *22*,755-765.

[20] D. Khatua, J. Dey, *J. Phys. Chem. B* **2007**, *111*, 124-130.

[21] Y. Dong, B. Xu, J. Zhang, X.Tan, L. Wang, J. Chen, H. Lv, S. Wen, B. Li, L. Ye, B. Zou, W. Tian, *Angew. Chem. Int. Ed.* **2012**, *51*, 10782-10785; *Angew. Chem.* **2012**, *124*, 10940-10943.

[22] Y. Zhou, D. Yan, *Chem. Commun.* **2009**, 1172-1188.

[23] W. Lyu, J. Feng, W. Yan, C. F. J. Faul, *J. Mater. Chem. C* **2015**, *3*, 11945-11952.

This article is protected by copyright. All rights reserved.

Accepted Manuscript

[24] M. S. Dresselhausa, G. Dresselhausc, A. Joriob, A.G. Souza Filhob, R. Saito, *Carbon* **2002**, *40*, 2043-2061.

[25] H. Zhu, M. J. McShane, *J. Am. Chem.Soc.* **2005**, *127*, 13448-13449.

[26] a) D. Mandal, M. Ghosh, S. Maiti, K. Das, P. K. Das, *Colloids Surf., B.* **2014**, *113*, 442 449; b) N. Nakayama-Ratchford, S. Bangsaruntip, X. Sun, K. Welsher, H. Dai, *J. Am. Chem.Soc.* **2007**, *129*, 2448-2449.

[27] Y. Shai, D. Bach, A. Yanovsky, *J. Biol. Chem.* **1990**, *265*, 20202-20209.

[28] a) M. Ghosh, S. Brahmachari, P. K. Das, *Macromol. Biosci.* **2014**, *14*, 1795-1806; b) Z. Chen, Z. Li, Y. Lin, M. Yin, J. Ren, X. Qu, *Biomaterials* **2013**, *34*, 1364-1371.

[29] S. Brahmachari, M. Ghosh, S. Dutta, P. K. Das, *J. Mater. Chem. B* **2014**, *2*, 1160-1173.

[30] M. B. Hansen, S. E. Nielsen, K. Berg, *J. Immunol. Methods* **1989**,*119*, 203-210.

[31] F. Wang, J. Liu, *Nanoscale* **2013**, *5*, 12375-12382;

[32] O. Regev, Y. Barenholz, S. Peretz, D. Zucker, Y. B. Felsen, *Future Med. Chem.* **2013**, *5*, 503-505.

Accepted Manuscript

This article is protected by copyright. All rights reserved.

10.1002/chem.201703452

Table 1. Steady-state fluorescence anisotropy (*r*) of DPH with varying concentrations of **T1** in DMSO−water (2:1, v/v) and **T1S** in water

Concentration/ mg/mL	*r*-values	
	T1	**T1S**
2	0.08	0.07
4	0.08	0.07
8	0.14	0.13
10	0.16	0.15
16	0.19	0.15
20	0.19	0.15

Accepted Manuscript

This article is protected by copyright. All rights reserved.

10.1002/chem.201703452

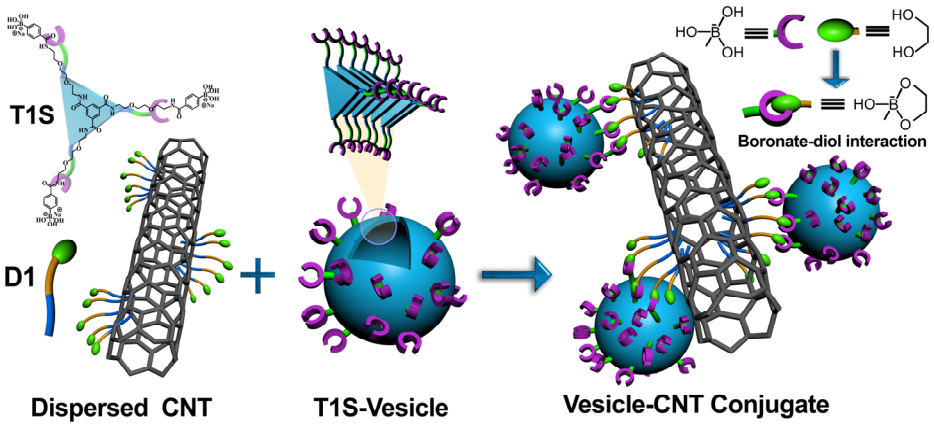

Scheme 1. Schematic representation of the formation of supramolecular vesicle-CNT conjugate through boronate-diol covalent linkage.

Accepted Manuscript

This article is protected by copyright. All rights reserved.

10.1002/chem.201703452

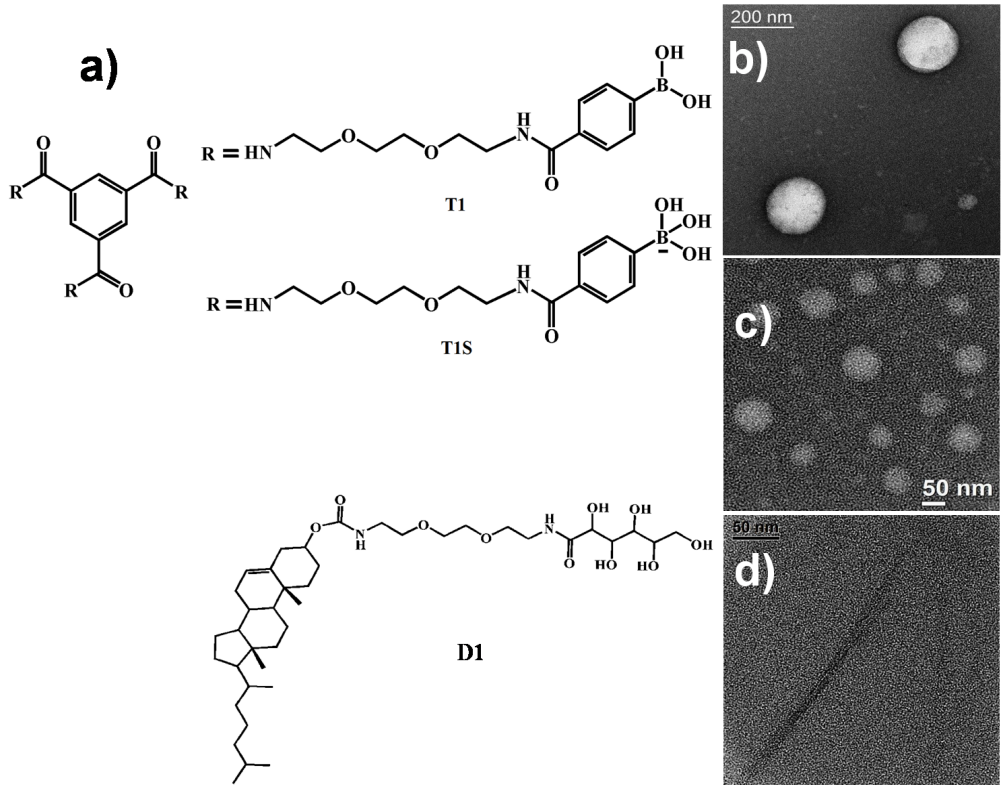

Figure 1. a) Structure of synthesized triskelion amphiphiles and dispersing agent. Negatively stained TEM images of b) **T1** prepared in DMSO-water (2:1, v/v) c) **T1S** prepared in water and d) dispersed CNT in water by **D1**.

This article is protected by copyright. All rights reserved.

Accepted Manuscript

10.1002/chem.201703452

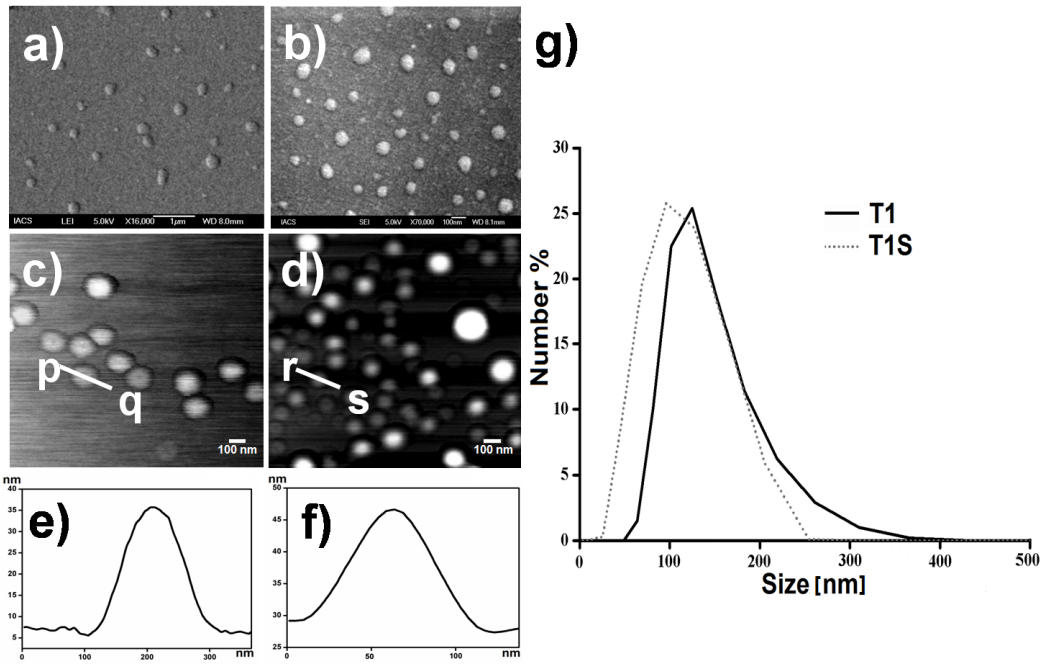

Figure 2. FESEM images of a) **T1**-vesicles prepared in DMSO-water (2:1, v/v) b) **T1S**-vesicles prepared in water, AFM images of c) **T1**-vesicles prepared in DMSO-water (2:1, v/v) (inset shows height profile along p-q) and d) **T1S**-vesicles prepared in water (inset shows height profile along r-s). e) Size distribution profile from DLS for **T1** and **T1S** vesicles.

Accepted Manuscript

This article is protected by copyright. All rights reserved.

10.1002/chem.201703452

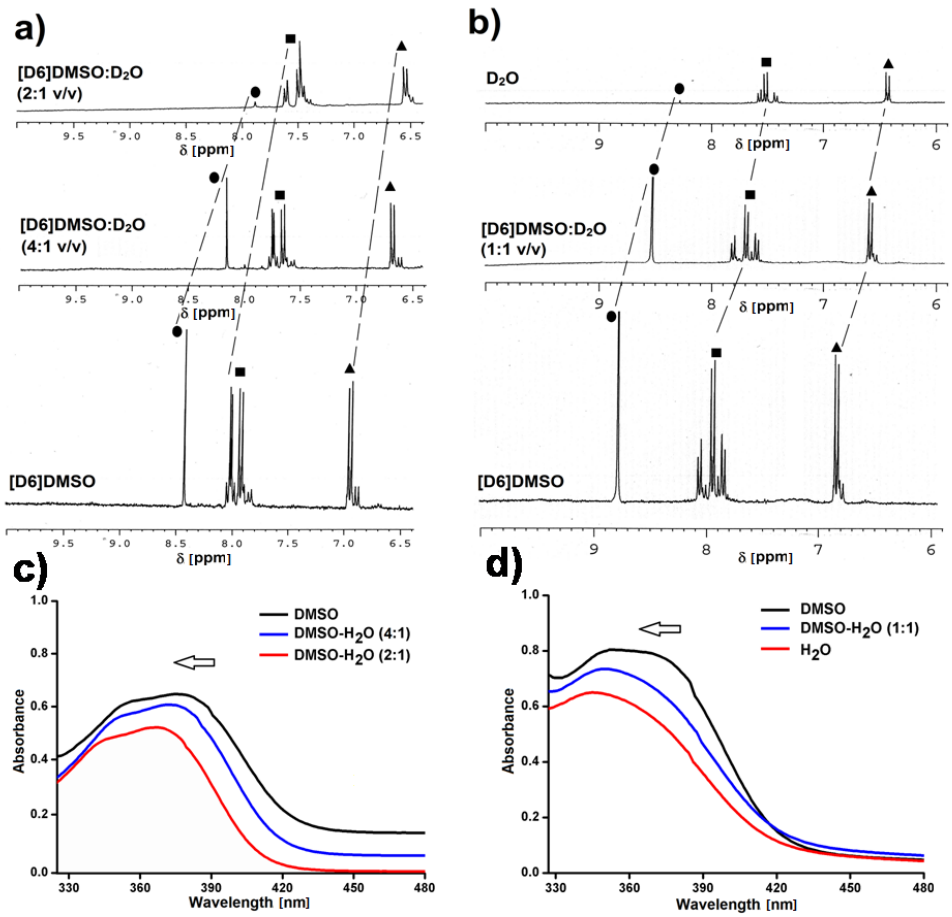

Figure 3. Solvent dependent ^{1}H-NMR spectra of a) **T1** and b) **T1S** showing the shift of aromatic protons of trimesic acid (●) and phenylboronic acid (■,▲). UV-Vis spectra of ANS doped c) **T1** and d) **T1S** in different solvent systems.

Accepted Manuscript

This article is protected by copyright. All rights reserved.

10.1002/chem.201703452

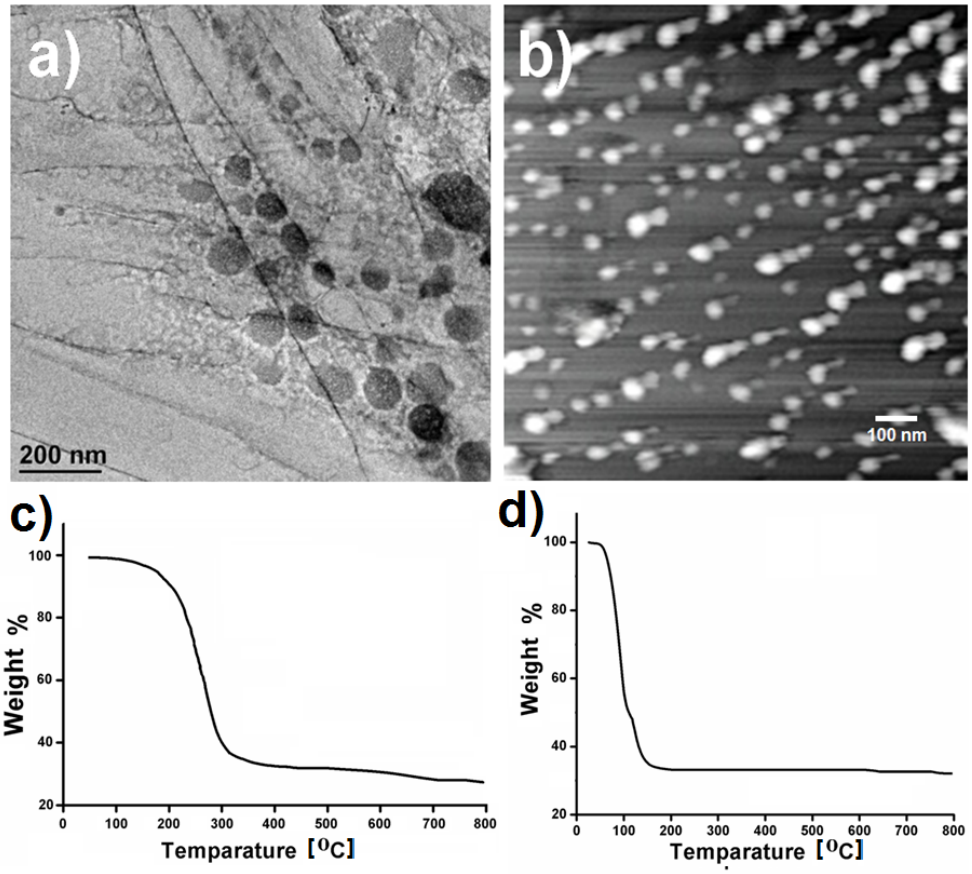

Figure 4. a) Negatively stained TEM b) AFM images of **T1S**-vesicle-**D1**-CNT conjugate. Thermogravimetric analysis (TGA) plots of c) **D1**-CNT and d) **T1S**-vesicle-**D1**-CNT conjugate.

This article is protected by copyright. All rights reserved.

Accepted Manuscript

10.1002/chem.201703452

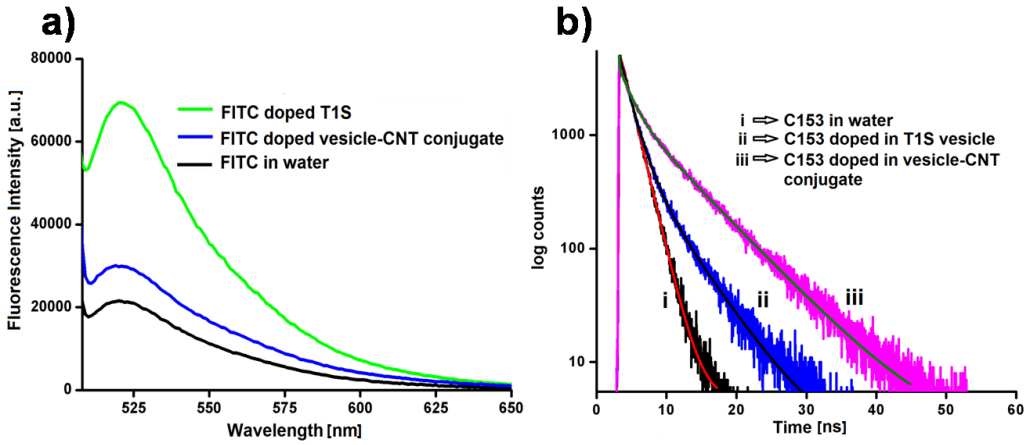

Figure 5. a) Fluorescence spectra of FITC in water, **T1S**-vesicle and **T1S**-vesicle-**D1**-CNT conjugate in water b) Decay curves of free C153 in water and encapsulated in **T1S**-vesicle and **T1S**-vesicle-**D1**-CNT conjugate prepared in water (excitation wavelength = 405 nm).

Accepted Manuscript

This article is protected by copyright. All rights reserved.

10.1002/chem.201703452

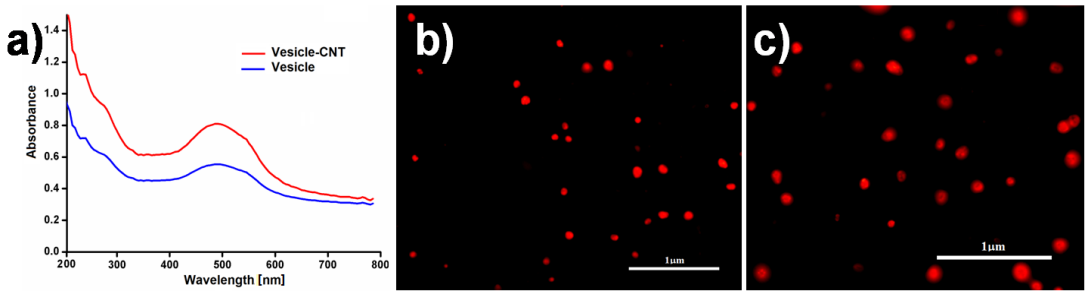

Figure 6. a) UV-Vis spectra of loaded doxorubicin in **T1S**-vesicle-**D1**-CNT conjugate, **T1S**-vesicle and fluorescence microscopic images of doxorubicin encapsulated b) **T1S**-vesicle and c) **T1S**- vesicle-**D1**-CNT conjugate.

Accepted Manuscript

This article is protected by copyright. All rights reserved.

10.1002/chem.201703452

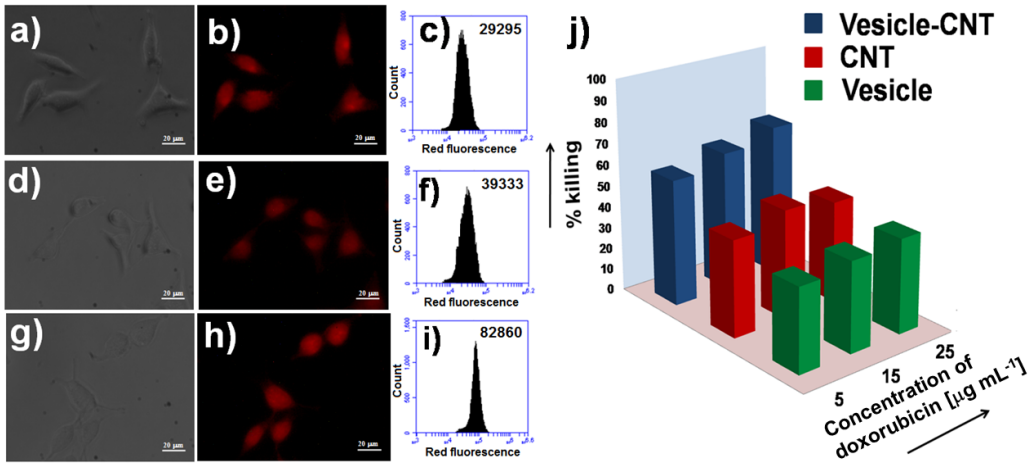

Figure 7. Bright field and fluorescence microscopic images of B16F10 cells after 6 h incubation with doxorubicin loaded (a,b) **T1S**-vesicle, (d,e) **D1**-CNT, (g,h) **T1S**-vesicle-**D1**-CNT conjugate. Corresponding flow cytometric histogram plots for (c) **T1S**-vesicle, (f) **D1**-CNT, (i) **T1S**-vesicle-**D1**-CNT conjugate and in all the flow cytometry plots the x-axis denotes the doxorubicin fluorescence intensity. The mean fluorescence values are given in the inset. (j) % Killing of B16F10 cells incubated with doxorubicin loaded **T1S**-vesicle, **D1**-CNT, **T1S**-vesicle-**D1**-CNT conjugate for 12 h with varying doxorubicin concentration. Percent errors are within ±5% in triplicate experiments.

Accepted Manuscript

This article is protected by copyright. All rights reserved.

10.1002/chem.201703452

Graphical Abstract

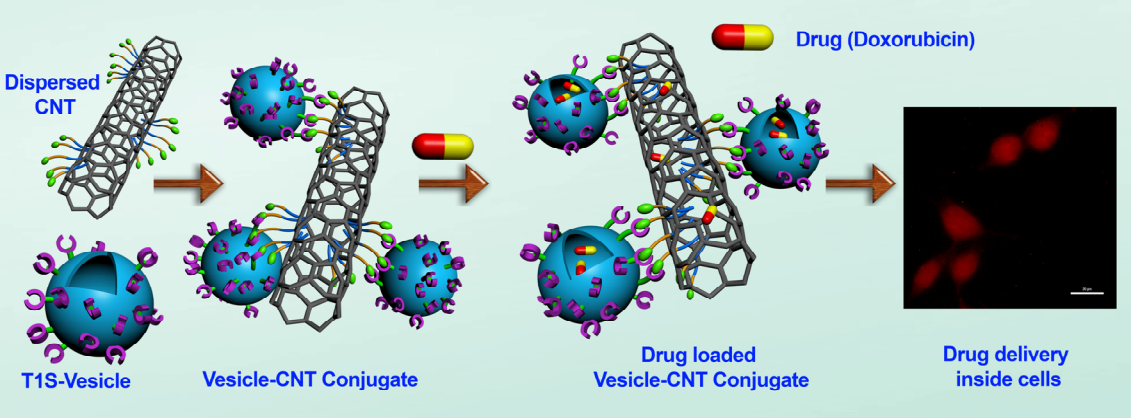

A vesicle-CNT conjugate was developed with facile combination of supramolecular self-assemblies of phenylboronic acid appended trimesic acid based monolayered vesicles and cholesterol based glucose functionalized CNT dispersion using simple boronate-diol covalent linkage. This vesicle-CNT conjugate showed superior biocompatibility, enhanced drug loading ability and improved proficiency in cellular transportation.

Keywords: Boronate-diol interaction, drug loading and delivery, monolayered vesicle, supramolecular self-assembly, vesicle-CNT conjugate

Accepted Manuscript

This article is protected by copyright. All rights reserved.